Schottky barrier heights, carrier density, and negative electron affinity of hydrogen-terminated diamond

K. Tsugawa,[1,2,*] H. Noda,[1] K. Hirose,[3] and H. Kawarada[1]

[1]*School of Science and Engineering, Waseda University, 3-4-1 Ohkubo, Shinjuku-ku, Tokyo 169-8555, Japan*

[2]*Nanotube Research Center, National Institute of Advanced Industrial Science and Technology (AIST), Tsukuba Central 5, 1-1-1 Higashi, Tsukuba, Ibaraki 305-8565, Japan*

[3]*Institute of Space and Astronautical Science (ISAS), Japan Aerospace Exploration Agency (JAXA), 3-1-1 Yoshinodai, Sagamihara, Kanagawa 229-8510, Japan*

(Received 21 May 2009; published 8 January 2010)

Chemical trends of Schottky barrier heights of ten kinds of metal contacts on hydrogen-terminated diamond (001) surfaces are estimated from the temperature dependence of their current-voltage characteristics. In addition to the measurements, the interface of the metal/hydrogen-terminated diamond is theoretically modeled including the carrier density of the surface conductive layer and the electron-affinity variation from the clean surface of the hydrogen-terminated diamond. Based on the model, a relation among the carrier density, the electron affinity variation, and the barrier heights are derived. The relation explains well experimental results of and other than the present work.

DOI: 10.1103/PhysRevB.81.045303 PACS number(s): 73.30.+y

I. INTRODUCTION

Surfaces of diamonds prepared by chemical vapor deposition (CVD) technique are terminated by hydrogen. Despite undoping, the hydrogen-terminated surface of diamond exhibits *p*-type surface conduction[1] in a subsurface region of ~10 nm in depth.[2,3] The surface conduction disappears by oxidation and consequently the surface becomes insulating.[4,5] Furthermore, Schottky and ohmic metal contacts are easily formed on the same surface by selecting kinds of metals.[6,7] Utilizing this nature, electronic devices such as, in particular, metal-semiconductor field-effect transistors (MESFETs) have been fabricated on hydrogen-terminated diamond surfaces.[2,5,6,8] Especially in microwave power electronics, the performance has been improving since a diamond microwave MESFET reported for the first time in 2001.[9] Recently, cut-off frequencies for the current and power gains, f_T and f_{max} have reached 45 and 120 GHz, respectively. At the same time, an output power density of 2.1 W/mm at 1 GHz has been realized.[8]

In spite of its potential for applications of the surface conduction on the hydrogen-terminated diamond, the detail understanding of its origin and transport properties is not adequate and remains still controversial at present.[10–12] Schottky barrier heights (SBHs) of metal/oxygenated-diamond contacts have been reported to be comparatively high (1–2 eV) and independent of the metal work function or the metal electronegativity.[6,13–18] The results suggest that the Fermi level at the interface is pinned in the band gap of diamond. This agrees with a result of x-ray photoemission spectroscopy that the Fermi level of the oxygenated surface is pinned at 1.7 eV above the valence-band maximum (VBM).[19] In contrast to this, the Fermi-level pinning is reduced at the interface of the metal/hydrogen-terminated diamond. In our previous work,[6,20] barrier heights of various metal contacts on the hydrogen-terminated diamond (001) were estimated from their current-voltage (*I-V*) characteristics using high-quality point-contact diodes. A strong correlation between the barrier heights and metal electronegativities was observed. In addition, ohmic characteristics were obtained in metals with comparably high electronegativities, such as Pt and Au. The results indicate that the Fermi level at the interface is not strongly pinned. However, the barrier heights were obtained by a rough estimation based on assumed contact areas, which were probably overestimated.

The hydrogen-terminated surface of diamond exhibits negative electron affinity (NEA) (Refs. 21–24) while those of clean and oxygen-terminated surfaces are positive. This nature indicates vast potentials for electronic applications such as cold cathode emitters, etc.

The electron affinity of diamond varies with its surface structure. The variation reaches up to 3 eV from the oxygen-terminated surface to the hydrogen-terminated surface.[24] The NEA of the hydrogen-terminated surface is related to its surface C-H dipoles.[23,24] On the other hand, the interfacial dipoles affect the barrier height of an interface.[25] Hence the electron-affinity variation should affect barrier heights. However, very few arguments have appeared up to the present.

In this work, the interfaces of metal/hydrogen-terminated diamond contacts are modeled including the carrier density of the surface conductive layer and the electron-affinity variation from the clean surface. Based on the model and experimentally obtained barrier heights, the carrier density and the electron affinity of the hydrogen-terminated diamond surface are discussed. In addition, the Fermi-level position of the free surface is also discussed.

II. EXPERIMENT

The starting materials were homoepitaxial diamond films deposited by microwave plasma-assisted CVD technique on high-pressure high-temperature synthetic Ib diamond (001) substrates ($1.5 \times 2.0 \times 0.3$ mm^3 in size). The reaction gases were $CH_4(2.25\%)/O_2(0.75\%)$ diluted with H_2 in a total gas flow of 100 sccm and under a total pressure of 35 Torr. The substrate temperature was raised up to 900 °C by plasma

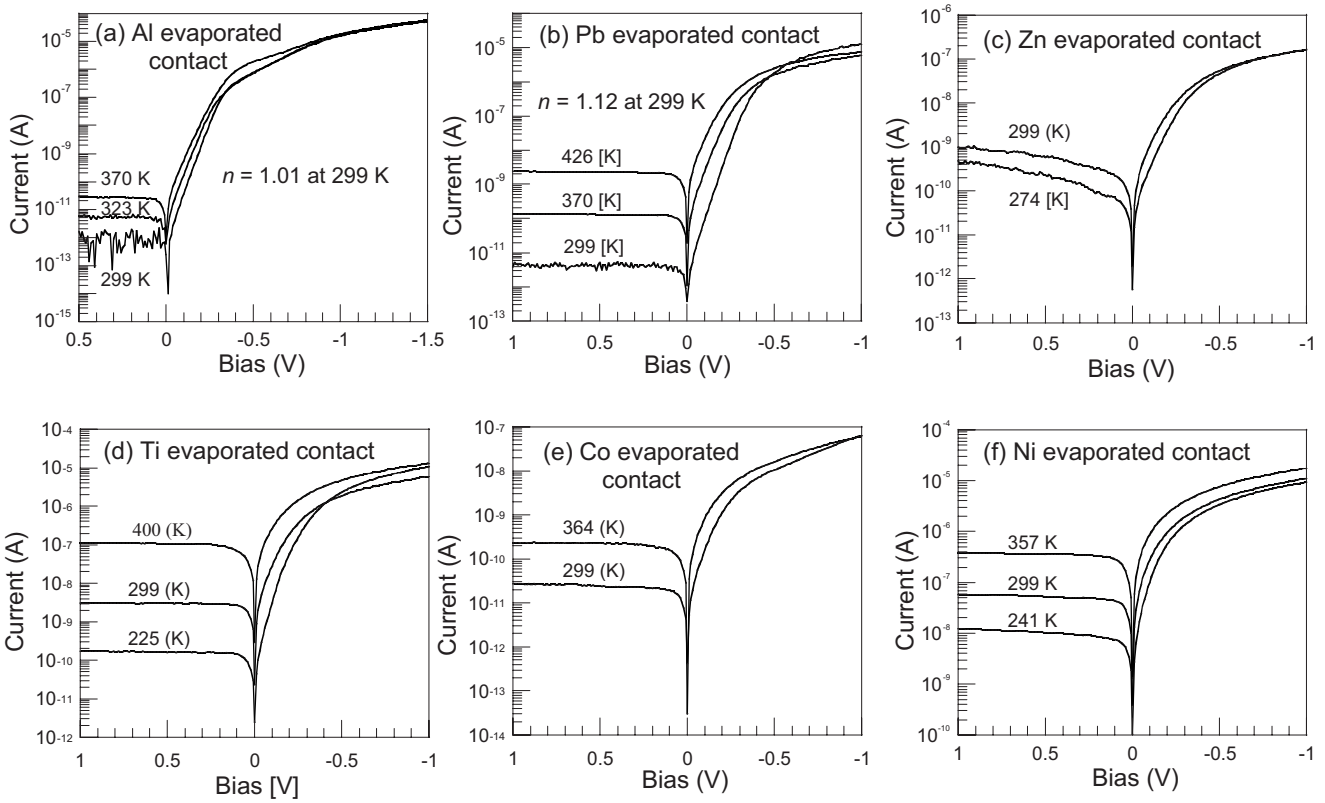

FIG. 1. Typical *I-V* characteristics of evaporated metal contacts on the hydrogen-terminated diamond (001), measured at various substrate temperatures: (a) an Al, (b) Pb, (c) Zn, (d) Ti, (e) Co, and (f) Ni contacts.

during the deposition. The deposition time was normally 3 h and the estimated thickness of the deposited film is approximately 1 μm. A hydrogen-plasma treatment followed the deposition process to obtain reproducibly complete hydrogen termination and the *p*-type surface conduction. In this treatment, the samples were exposed to pure hydrogen plasma and were cooled down to room temperature in a pure hydrogen ambience.

Metal contacts on the homoepitaxial diamonds were prepared by vacuum thermal evaporation of metals at room temperature. Ten kinds of metals were deposited in dots (0.2 mm in diameter) onto the homoepitaxial diamond films, such as Al, Pb, Zn, Ti, Co, Ni, Cu, Ag, Au, and Pt. The samples were mounted on a brass holder with Ag paste to obtain an ohmic contact between the surface conductive layer and the holder. A Hewlett-Packard model 4155A pA meter and voltage source was used to record *I-V* characteristics. Temperatures of the samples were controlled from room temperature to 300 °C. The *I-V* measurements were controlled automatically by a personal computer.

III. RESULTS

Six metal contacts of the ten exhibit Schottky characteristics, such as Al, Pb, Ti, Zn, Co, and Ni, whereas the Cu, Ag, Au, and Pt contacts indicate ohmic characteristics. Figure 1 demonstrates typical *I-V* characteristics at various substrate temperatures of the six types of Schottky contacts on the hydrogen-terminated diamond (001). Apparent increases in the reverse-bias current with rising temperatures are observed for all the contacts in the figure. The Al contact in Fig. 1(a), deserving special note, exhibits an ideality factor n of 1.01 at 299 K (room temperature), which coincides with a sufficiently ideal Schottky contact to evaluate its barrier height by using the thermionic emission theory.

In the thermionic emission theory, the forward current I_F and the reverse saturation current I_S of a Schottky contact at a temperature T obey the following equations:

$$\ln(I_F/T^2) = \ln(SA^{**}) - q(\phi_{bp} - V_F)/kT, \tag{1}$$

$$\ln(I_S/T^2) = \ln(SA^{**}) - q\phi_{bp}/kT. \tag{2}$$

Here S, A^{**}, q, and k are the contact area, the effective Richardson constant, the electron charge, and the Boltzmann constant, respectively. By plotting $\ln(I/T^2)$ as a function of $1/T$, a linear relationship is obtained as expected from Eqs. (1) and (2) (Richardson plots). The dependence of $\ln(I_F/T^2)$ on $1/T$ [Eq. (1)] for the Al contact, the *I-V* curves of which are displayed in Fig. 1(a), is shown in Fig. 2(a). In this case, the thermionic emission theory describes well the current-transport mechanism of the diode due to its excellent ideality factor (1.01) and the linearity of the Richardson plots. The barrier height of the Al/diamond contact is evaluated from the gradient of a least-square fit of the Richardson plots, and consequently it results in 0.59 eV. This value is much lower than those reported by other group (1.4–1.6 eV).[16,26,27] However, it is quite close to the results of contact potential

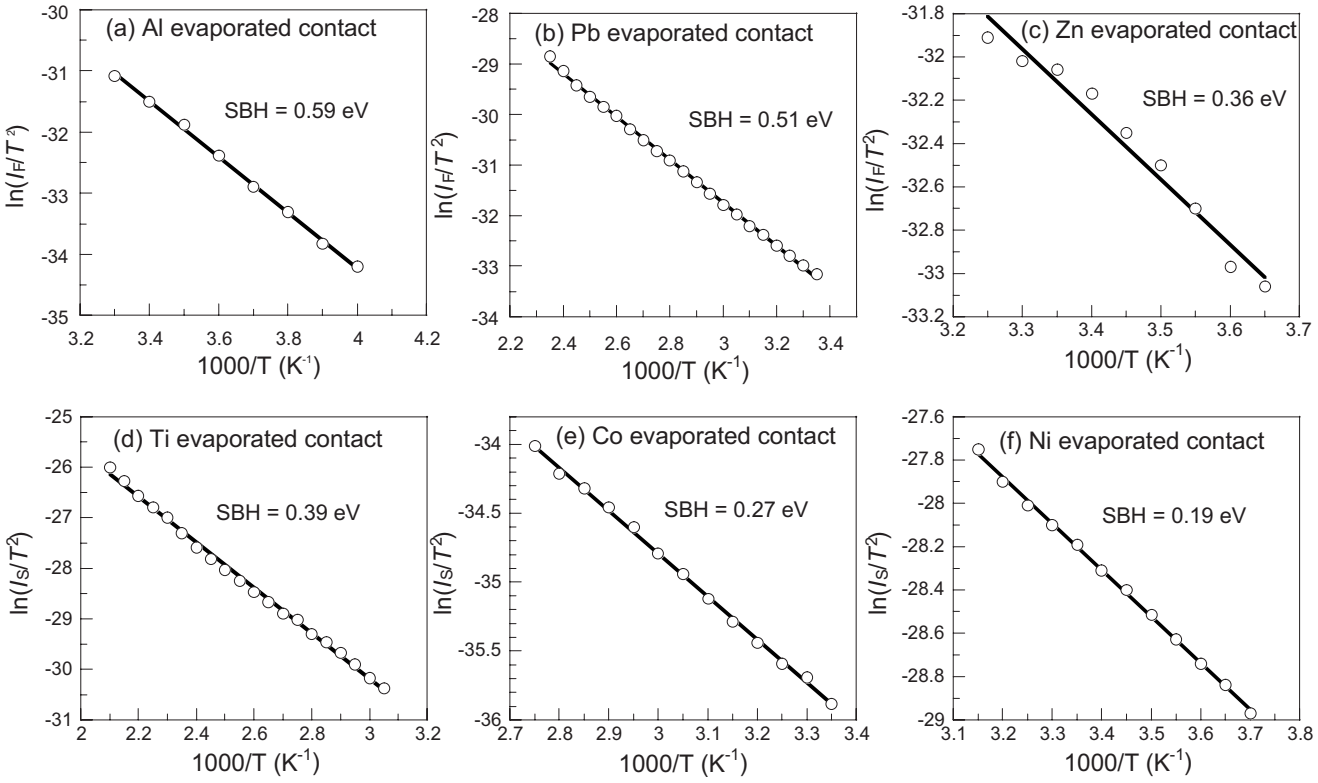

FIG. 2. Richardson plots of the Schottky contacts, the *I-V* characteristics of which are shown in Fig. 1: (a) the Al, (b) Pb, (c) Zn, (d) Ti, (e) Co, and (f) Ni contacts, In (a), (b), and (c), the plots are obtained by the temperature dependence of forward current at applied voltages of (a) −200 mV, (b) −140 mV, and (c) −100 mV. In (d), (e), and (f), the plots are yielded by the temperature dependence of reverse saturation current at an applied voltage of +350 mV for all the three. SBHs are extracted from the gradients of least-square fits using Eq. (1) for (a), (b), and (c); and using Eq. (2) for (d), (e), and (f).

difference measurements [0.6 (Ref. 28) and 0.57 eV (Ref. 29)].

One reason for the large difference of the barrier height of the Al contact from the previously reported values is the difference in estimation methods of the barrier heights. In the literatures,[16,27] a field and thermionic-field emission theory including tunneling processes by Padovani and Stratton[30] was used to estimate barrier heights from *I-V* characteristics. The Padovani-Stratton[30] model assumes an impurity concentration in the semiconductor, heavy doping in particular, and tunneling processes across a triangle-shaped potential barrier. However, the diamond layer is not doped and no such potential barrier at the interface exists for the metal/diamond contact here as illustrated in Fig. 3(b). Hence the Padovani-Stratton model is unsuitable for the estimation of barrier heights of metal contacts on the hydrogen-terminated undoped diamond. In fact, by using the conventional thermionic emission theory used in the present work, a barrier height of 0.6 eV has been obtained for the Al contact.[16] This value is close to the result of this work.

As another reason, the difference in preparation processes can be considered. All the samples in the literatures[16,26,27] were annealed in vacuum before *I-V* measurements. This process possibly changes barrier heights, judging from a theoretical analysis in the present work. The details are discussed later.

The same process as the Al contact has been applied to the others, namely, Pb, Zn, Ti, Co, Ni, Cu, Ag, Au, and Pt. In the case of the Pb contact, its *I-V* characteristics shown in Fig. 1(b) also indicate a good ideality factor of 1.12. The Schottky barrier height is estimated at 0.51 eV from the Richardson plots in Fig. 2(b). Likewise, for the Zn contact in Figs. 1(c) and 2(c), a barrier height of 0.36 eV is obtained. For the Ti, Co, and Ni contacts in Figs. 1(d)–1(f), respectively, the reverse saturation current I_S has been examined to avoid the effect of series resistance in the forward-bias region [Eq. (2)] because of their small rectifying ratios as shown in Figs. 1(d)–1(f). The estimated barrier heights of the Ti, Co, and Ni contacts, respectively, are 0.39, 0.27, and 0.19 eV. In the cases of the Cu, Ag, Au, and Pt contacts, their barrier heights are hardly determined due to their low value of near zero, i.e., they exhibit ohmic characteristics in the temperature range of the measurements. The results indicate that metals with relatively small electronegativities (Pauling's electronegativity $X_m < 1.9$), such as Pb, Al, Ti, Zn, and Co, exhibit good Schottky characteristics and high barrier heights. On the other hand, metals with high electronegativities ($X_m \geq 1.9$), such as Cu, Ag, Au, and Pt, form ohmic contacts on the hydrogen-terminated diamond. This implies that the boundary between Schottky and ohmic contacts exists at around an electronegativity of 1.9 in Pauling's scale. The ohmic characteristics of the Au or Pt contacts on the hydrogen-terminated surface agree with previously reported work.[6,7,18,20]

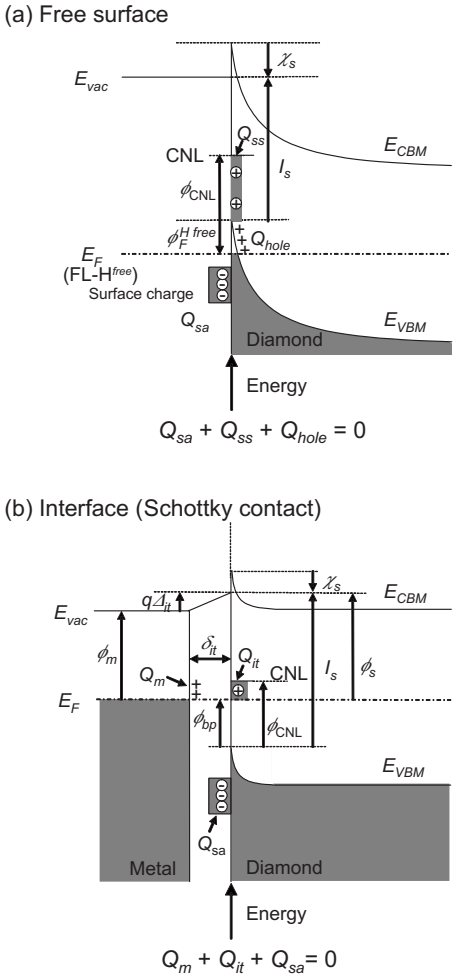

FIG. 3. Band diagrams (a) at the free surface of the hydrogen-terminated undoped diamond and (b) at the interface between a metal and the hydrogen-terminated undoped diamond. Positive quantities are indicated by upward arrows while downward arrows indicate negative quantities.

IV. DISCUSSION

A. Interface modeling for analysis

Before discussing the experimental results, the interface between metal and hydrogen-terminated undoped diamond is modeled for analysis. This system has peculiar characteristics different from other metal/semiconductor interfaces, such as the *p*-type surface conduction on the diamond surface despite undoping and the NEA.[23,24] Considering their effects, the interface is modeled based on the popular manner established by Cowley and Sze[31] and the metal-induced gap states(MIGS)-and-electronegativity model by Mönch.[32]

In the beginning, negative surface charge, with an area density of Q_{sa}, is assumed to exist near the VBM. This assumption is adopted considering an adsorbate layer of the transfer doping model,[10] ionized acceptor-type surface states or defects,[19,33] or others. Regardless of models for the origin of the surface conduction on the hydrogen-terminated diamond surface, the negative surface charge should exist below the Fermi level at the interface. Figure 3(a) schematically shows a band diagram of the hydrogen-terminated free surface before the formation of a contact. The NEA of the hydrogen-terminated diamond surface is included in the diagram. The surface charge is taken into the band line up and placed below the Fermi level E_F with a constant density per unit area of N_{sa}. This signifies that the adsorbate layer or the surface acceptors are completely charged. This assumption is adequately reasonable at room temperature.[34,35] Thus the surface charge is negative and has a constant area density of Q_{sa}, which is written as

$$Q_{sa} = -qN_{sa}. \tag{3}$$

In addition, the thickness of the surface charge layer is assumed to be atomic dimension.[2,3] At the free surface, Q_{sa} should be in balance with the net charge of surface states Q_{ss} and the charge of holes accumulated at the surface Q_{hole}^{acc} to satisfy the local charge neutrality at the surface

$$Q_{sa} + Q_{ss} + Q_{hole}^{acc} = 0. \tag{4}$$

The Fermi level at the hydrogen-terminated surface is located below the VBM.[28] Hence the surface states in the band gap below the charge-neutrality level (CNL) is positively charged while those above the CNL are neutral. That is to say, the net charge of the surface states is positive. This leads to $-Q_{sa} > Q_{hole}^{acc}$. Note N_{sa} corresponds to the carrier (hole) sheet density and Q_{hole}^{acc} is the area charge density of accumulated holes out of it.

Figure 3(b) depicts a band diagram of a metal/hydrogen-terminated undoped diamond interface after a Schottky contact formation. The metal and the diamond are assumed to be separated by an interfacial dielectric layer with a thickness of δ_{it} and a dielectric constant of ε_i. This type of interface model[31,36] has been frequently used to analyze metal/semiconductor interfaces. According to the MIGS concept,[37,38] interface states at the diamond side arise out of the penetration of the wave function of the metal electrons. Hence the density of the interface states is expected to be larger than the density of the surface states at the free surface. Hereafter, the interface states of the diamond side at the interface of the contact are differentiated from the surface states at the free diamond surface by the words "interface" and "surface." After the contact formation, the charges on the diamond side are Q_{sa} and the net charge of the interface states Q_{it}. They should be balanced with the interface charge on the metal side Q_m. In this case, holes on the diamond side are depleted ($Q_{hole}^{acc} \sim 0$) and the space charge by ionized impurities in the depletion region is zero due to the undoping of the diamond. This generates a deep depletion region beneath the contact, from the interface into the deep inside of the diamond. This is the two-dimensional (2D) nature of the surface conductive layer of the hydrogen-terminated diamond depicted by numerical calculations in the literature[3] and the experimentally observed periphery effects.[39,40] Eventually, the local charge neutrality at the interface is

$$Q_m + Q_{it} + Q_{sa} = 0. \tag{5}$$

In discussing metal/semiconductor interfaces, the concept of the CNL (Ref. 31) of interface states is essential to determine the barrier heights. The net charge of the interface states is determined by the position of the Fermi level with respect to

the CNL. The interface states with larger energies than the CNL are acceptorlike while ones with smaller energies are donorlike. In other words, Q_{it} is negative when the Fermi level is positioned above the CNL and is positive with the Fermi level below the CNL. Thus the coincidence of the Fermi level and the CNL means charge neutral of the interface states and zero-charge transfer between the metal and the semiconductor. Using ϕ_{CNL}, the energy position of the CNL with respect to the VBM, the net charge density per unit area of the interface states Q_{it} is derived by

$$Q_{it} = q\int_{\phi_{bp}}^{\phi_{\mathrm{CNL}}} D_{it}(E)\mathrm{d}E.$$

Here ϕ_{bp} is the barrier height and D_{it} denotes the density of the interface states. For simplicity, assuming a continuum of interface states with a constant density of states D_{it} across the band gap,[31] one obtains

$$Q_{it} = qD_{it}(\phi_{\mathrm{CNL}} - \phi_{bp}). \tag{6}$$

On the other hand, the parallel-plate capacitor between the metal and the diamond with a potential drop of Δ_{it} shown in Fig. 3(b) yields

$$Q_m = \frac{\varepsilon_i\varepsilon_0\Delta_{it}}{\delta_{it}} = \frac{\varepsilon_i\varepsilon_0}{q\delta_{it}}(I_s - \phi_{bp} - \phi_m). \tag{7}$$

Here ε_0, I_s, and ϕ_m are, respectively, the permittivity of vacuum, the ionization potential of the diamond, which denotes the energy of the VBM (E_{VBM}) with respect to the vacuum level, and the work function of the metal. Substituting Eqs. (3), (6), and (7) into Eq. (5) and rearranging it, one obtains

$$\phi_{bp} = I_s - \phi_m + \frac{q^2\delta_{it}D_{it}}{\varepsilon_i\varepsilon_0}(\phi_{\mathrm{CNL}} - \phi_{bp}) - \frac{q^2\delta_{it}}{\varepsilon_i\varepsilon_0}N_{sa}. \tag{8}$$

As one can see in Fig. 3(b), the barrier height ϕ_{bp} is written by using the potential drop across the interfacial layer Δ_{it} as

$$\phi_{bp} = I_s - \phi_m - q\Delta_{it}. \tag{9}$$

Comparing Eqs. (8) and (9), one obtains

$$q\Delta_{it} = q\Delta_{gs} + q\Delta_{sa} = -\frac{q^2\delta_{it}D_{it}}{\varepsilon_i\varepsilon_0}(\phi_{\mathrm{CNL}} - \phi_{bp}) + \frac{q^2\delta_{it}}{\varepsilon_i\varepsilon_0}N_{sa}. \tag{10}$$

Here Δ_{gs} and Δ_{sa} are defined as

$$q\Delta_{gs} = -\frac{q^2\delta_{it}D_{it}}{\varepsilon_i\varepsilon_0}(\phi_{\mathrm{CNL}} - \phi_{bp}),$$

$$q\Delta_{sa} = \frac{q^2\delta_{it}}{\varepsilon_i\varepsilon_0}N_{sa}. \tag{11}$$

Δ_{it} can be considered as the difference in the vacuum level just outside the diamond from the one just out side of the metal. At the same time, it represents a deviation from the Schottky-Mott relationship $\phi_{bp}=I_s-\phi_m$. Δ_{it} consists of two terms, such as Δ_{gs} and Δ_{sa}, as seen in Eqs. (10) and (11). Δ_{gs} expresses the Fermi-level pining. It works as negative feedback to converge the Fermi level to the CNL.[41] The driving force of the convergence becomes stronger with increasing interface state density D_{it}. On the other hand, Δ_{sa} represents the contribution of the surface charge Q_{sa} to the barrier height. This effect works as constant shifts on the barrier heights to be reduced due to its constant density of negative charge.

Rearranging Eq. (8) gives

$$\phi_{bp} = S_\phi(I_s - \phi_m) + (1 - S_\phi)\left(\phi_{\mathrm{CNL}} - \frac{N_{sa}}{D_{it}}\right) \tag{12}$$

with the slope parameter

$$S_\phi = -\frac{\partial\phi_{bp}}{\partial\phi_m} = \left(1 + \frac{q^2\delta_{it}D_{it}}{\varepsilon_i\varepsilon_0}\right)^{-1}. \tag{13}$$

S_ϕ is experimentally obtained by $S_\phi=-\partial\phi_{bp}/\partial\phi_m$ (Refs. 31 and 36) and the barrier heights depend linearly on the metal-work functions through $-S_\phi$ as indicated by Eq. (12). From Eq. (13), $D_{it}\approx 0$ gives $S_\phi\approx 1$. In this case, the Schottky-Mott rule is recovered as one can see in Eq. (12). In contrast, a large D_{it} that indicates $S_\phi\approx 0$ gives $\phi_{bp}=\phi_{\mathrm{CNL}}-N_{sa}/D_{it}$. In other words, the Fermi level is pinned at below the CNL by N_{sa}/D_{it}. Equation (12) suggests that the barrier-height variation by N_{sa} is written as

$$\Delta\phi_{bp}^{sa} = -(1 - S_\phi)\frac{N_{sa}}{D_{it}}. \tag{14}$$

This barrier height reduction is the same value as fully charged interface defects with the area density of N_{sa}.[36]

In the simple Schottky-Mott picture of metal/semiconductor interfaces, The Schottky barrier height of an interface is defined as the energy difference between the ionization potential (E_{VBM} with respect to the vacuum level) of the semiconductor and the metal work function, when the semiconductor is doped p type. In characterizing the metal, however, the electronegativity X_m has been used rather than the work function ϕ_m. This preference for X_m rather than ϕ_m was led by the difference between the internal work function related to the electronegativity and the measured work function due to the additional electronic contribution from the surface dipole of the metal.[42,43]

The interface states at an ideal metal/semiconductor contact are identified with the continuum of the MIGS.[37,38] The barrier heights arise from charge transfer across the interface to satisfy the interface charge neutrality as discussed before. In generalizing Pauling's concept for small molecules, Mönch[32,44] has modeled the interface charge transfer by the electronegativity differences X_m-X_s of metals and a semiconductor. In consequence, he obtained the following equation for metal/p-type semiconductor interfaces:[32,44]

$$\phi_{bp} = \phi_0^* - S_x(X_m - X_s), \tag{15}$$

where ϕ_0^* is the zero-charge-transfer barrier height (the energy of the CNL with respect to the VBM, i.e., $\phi_0^*\equiv\phi_{\mathrm{CNL}}$ for ideal metal/semiconductor contacts). S_x is the slope parameter ($S_x=-\partial\phi_{bp}/\partial X_m$). X_m and X_s are the electronegativities of the metal and the semiconductor, respectively.

For metal contacts on the hydrogen-terminated diamond surface, the chemical trends of their barrier heights deviate from the MIGS line Eq. (15).[6,25] As one of origins of the deviation, Mönch[25] has taken the potential drop across the surface C-H dipole layer into account. In addition, Kawarada[6] has assumed acceptor-type interface states near the VBM as another origin of the deviation, the net effect of which is written as the same manner as Eq. (14).

In the concept of the MIGS-and-electronegativity model, the charge transfer across metal/semiconductor interfaces is determined by $X_m - X_s$. In other words, the charge density at the metal side Q_m and at the semiconductor side Q_s are expressed as

$$-Q_m = Q_s \propto X_m - X_s. \tag{16}$$

In our case here, from Fig. 3 and Eq. (5)

$$Q_s = Q_{it} + Q_{sa}. \tag{17}$$

If a dipole layer exists on the semiconductor side of the interface, the charge density of the dipole layer Q_{id} should be taken into account. Hence Eq. (17) becomes

$$Q_s = Q_{it} + Q_{sa} + Q_{id}. \tag{18}$$

In the interface C-H dipoles on the hydrogen-terminated diamond, the H atoms are positively charged while the C atoms are charged negative.[25] Hence the contribution of the dipole charge Q_{id} to the semiconductor (diamond) side is negative. According to Eq. (16), Q_s may not change regardless of the presence of Q_{id}. Since Q_{sa} is constant, the presence of Q_{id} yields a change in ΔQ_{it}, i.e.,

$$\Delta Q_{it} = -Q_{id}. \tag{19}$$

From Eqs. (6) and (19), one obtains a barrier-height variation $\Delta\phi_{bp}^{id}$ by the interface dipole layer as

$$-Q_{id} = \Delta Q_{it} = -qD_{it}\Delta\phi_{bp}^{id}. \tag{20}$$

Here $\Delta\phi_{bp}^{id} < 0$ due to $Q_{id} < 0$, i.e., the barrier heights are reduced by the interface dipole layer.

The unchanged Q_s regardless of the presence of Q_{it} means that the interface potential barrier Δ_{it} is not changed by Q_{id}. This indicates that the energy drop across the interface dipole layer $q\Delta_{id}$ is identical to the barrier-height reduction $\Delta\phi_{bp}$. Based on the idea discussed above by Mönch, barrier heights of Ag (Ref. 45) and Pb (Ref. 46) contacts on hydrogen-terminated Si(111) surfaces have been successfully explained.

Equation (19) suggests that the charge density of the interface C-H dipole layer Q_{id} does not affect the interface potential barrier Δ_{it}, namely, Δ_{id} exists on the outside of Δ_{it}. Since $q\Delta_{it}$ is the difference of the vacuum levels just outside the metal and the diamond, the vacuum level just outside the diamond is located at the opposite side of the dipole layer to the diamond side. This indicates that $q\Delta_{id}$ is equivalent to the shift in electron affinity from the clean surface.

This assumption has been also supported by experiments with other techniques. By using combining work-function measurements with photoelectron yield and core-level photoemission spectroscopy, Cui *et al.*[23] have found that the electron-affinity difference between the NEA hydrogen-terminated surface and the clean surface directly mirrors the potential drop across the surface C-H dipole layer for diamond (111) surfaces. In succession to them, in a similar manner, Maier *et al.*[24] have reached similar results for hydrogen-terminated diamond (001) surfaces.

Judging from these facts, the electron-affinity difference $\Delta\chi_s$ between the hydrogen-terminated and the clean diamond surfaces is identical to $q\Delta_{id}$. Thus one gets

$$\Delta\phi_{bp}^{id} = q\Delta_{id} = \Delta\chi_s = \chi_s^{Hterm} - \chi_s^{clean}. \tag{21}$$

Here χ_s^{Hterm} and χ_s^{clean} denote the electron affinity of the hydrogen-terminated and of the clean surfaces, respectively.

Considering both the effects of the surface charge and the interface dipoles, the total barrier-height variation is

$$\Delta\phi_{bp}^{sa} + \Delta\phi_{bp}^{id} = -(1 - S_\phi)\frac{N_{sa}}{D_{it}} + \Delta\chi_s = -S_\phi\frac{q^2\delta_{it}}{\varepsilon_i\varepsilon_0}N_{sa} + \Delta\chi_s. \tag{22}$$

Hence the MIGS line Eq. (15) is expected to become

$$\phi_{bp} = \phi_{\mathrm{CNL}} - S_\phi\frac{q^2\delta_{it}}{\varepsilon_i\varepsilon_0}N_{sa} + \Delta\chi_s - S_x(X_m - X_s). \tag{23}$$

In this case, ϕ_0^* in Eq. (15) is not identical to ϕ_{CNL} any longer, i.e.,

$$\phi_0^* = \phi_{\mathrm{CNL}} - S_\phi\frac{q^2\delta_{it}}{\varepsilon_i\varepsilon_0}N_{sa} + \Delta\chi_s. \tag{24}$$

In the MIGS-and-electronegativity model, the MIGS line Eq. (15) is derived from the correlation between the electronegativity X_s and the dielectric work function ϕ_{sd} of a semiconductor[32]

$$\phi_{sd} = E_{vac} - E_{\mathrm{CNL}} = I_s - \phi_{\mathrm{CNL}} = A_xX_s + B_x. \tag{25}$$

Here the parameters A_x and B_x are the same as those for polycrystalline metals, namely,

$$\phi_m = A_xX_m + B_x. \tag{26}$$

The dielectric work function is the energy of the CNL with respect to the vacuum level. For an intrinsic semiconductor, the Fermi level of a free surface coincides with the CNL in order to satisfy the local charge neutrality at the surface. In the electronegativity concept, no charge transfer through the interface occurs when the metal and the semiconductor have identical electronegativities. Likewise, no charge transfer occurs as long as the Fermi level is positioned at the CNL because no charges emerge at the interface due to the local charge neutrality.

The discussion about Eq. (19) implies that the dielectric work function of the hydrogen-terminated surface of diamond is equal to that of the clean surface. In other words, the Fermi-level position with respect to the vacuum level of the hydrogen-terminated surface is identical to that of the clean surface. This agrees well with experimental results in this work as discussed later. The energy position of the Fermi level on the hydrogen-terminated diamond surface is thought to be below the VBM (Ref. 28) as illustrated in Fig. 3(a). Here we define this Fermi level of the free hydrogen-

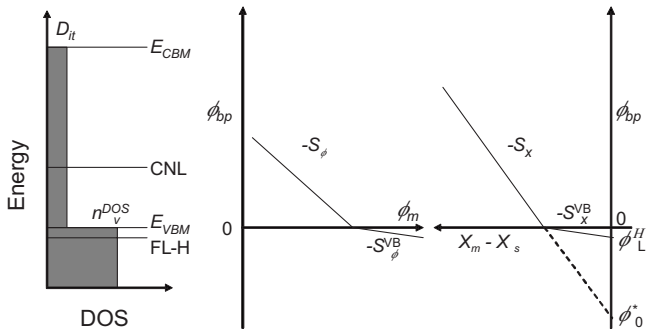

FIG. 4. A schematic diagram of the density-of-states energy distribution for the interface states and the valence band near the VBM. Corresponding MIGS lines of barrier heights against metal-work functions and electronegativity differences are also illustrated.

terminated diamond surface as FL-H^{free} and its energy position from the VBM as ϕ_L^{Hfree}. Likewise, we define the similar energy at a metal/diamond interface to FL-H^{free} as FL-H, the energy position of which is ϕ_L^H with respect to the VBM, i.e., no charge transfer occurs through the interface when the Fermi level is positioned at FL-H.

The carriers (holes) of the surface-conductive layer are activated completely above 70 K.[35] Hence, the surface-charge density N_{sa} is constant at room temperature. In addition, the free surface is neutral when the Fermi level coincides with FL-H^{free} due to the charge neutrality condition Eq. (4). Hence the net charge of the free surface is negative, vanishes, and becomes positive when the Fermi level is above, coincides with, and drops to below FL-H^{free}. This behavior is as if it were the CNL of gap states. Furthermore, for a metal/hydrogen-terminated diamond interface, no charge transfer across the interface occurs if the Fermi level is located at FL-H. However, note FL-H at the interface of a metal/diamond contact may be slightly different from FL-H^{free} of the free diamond surface. The density of interface states (MIGS) is considered to be larger than the density of surface states because the MIGS is induced by the penetration of electron wave functions from the metal into the semiconductor.[37] Since the density of states of the valence band near the VBM is supposed to be much larger than the density of the interface or the surface states, the difference is expected to be small and negligible. Thus Eq. (25) for the hydrogen-terminated diamond is

$$\phi_{sd} = I_s - \phi_L^H = A_x X_s + B_x. \tag{27}$$

If the Fermi level at the interface coincides with FL-H, namely, $\phi_m = \phi_{sd}$, no charge transfer occurs across the interface. Hence, one results in $X_m - X_s = 0$ in this case. This means that the MIGS line should pass through ϕ_L^H at $X_m - X_s = 0$. The MIGS line Eq. (23) is defined for $\phi_{bp} \geq 0$, however, since the slope parameter S_ϕ is determined by D_{it}, the density of the interface states within the band gap, as indicated by Eq. (13). For $\phi_{bp} < 0$, i.e., the Fermi level at the interface becomes below the VBM, the MIGS line should have a different slope parameter S_ϕ^{VB} from S_x, which is determined by the density of states of the valence band near the VBM in a similar manner to Eq. (13). This situation is schematically illustrated in Fig.4.

The accumulated holes in the surface conductive layer on the hydrogen-terminated diamond exhibit 2D behavior.[2,3,29,47] For a 2D hole system with parabolic bands, the density of states $n_v^{DOS}(E)$ is constant and does not depend on energy, which is given by

$$n_v^{DOS}(E) = n_v^{DOS} = \frac{m_h^*}{\pi\hbar^2}, \tag{28}$$

where m_h^* is the effective mass of holes.

Here, for simplicity, we proceed with classical manner by neglecting quantization effects in the 2D system.[29,47] From Eq. (13), the slope parameter S_ϕ^{VB} for $\phi_{bp} < 0$ is expected to be determined by

$$\begin{aligned} S_\phi^{VB} &= -\frac{\partial \phi_{bp}}{\partial \phi_m} \\ &= \left(1 + \frac{q^2 \delta_{it} n_v^{DOS}}{\varepsilon_i \varepsilon_0}\right)^{-1} \\ &= \left(1 + \frac{q^2 \delta_{it}}{\varepsilon_i \varepsilon_0} \frac{m_h^*}{\pi\hbar^2}\right)^{-1} (\phi_{bp} < 0). \end{aligned} \tag{29}$$

From the relationship Eq. (26), one gets

$$S_x^{VB} = -\frac{\partial \phi_{bp}}{\partial X_m} = A_x S_\phi^{VB} \quad \text{and} \quad S_x = A_x S_\phi. \tag{30}$$

If $\phi_{bp} = 0$ at $X_m = X_m^0$, Eq. (15) gives

$$X_m^0 - X_s = \frac{\phi_0^*}{S_x}. \tag{31}$$

Thus, from Fig. 4 and Eq. (29), one obtains

$$\phi_L^H = S_x^{VB}(X_m^0 - X_s) = \frac{S_x^{VB}}{S_x}\phi_0^* = \frac{A_x \phi_0^*}{S_x}\left(1 + \frac{q^2 \delta_{it}}{\varepsilon_i \varepsilon_0} \frac{m_h^*}{\pi\hbar^2}\right)^{-1}. \tag{32}$$

Hence, using Eq. (28), the area density of holes accumulated at the free surface p_{acc} is given by

$$p_{acc} \approx -n_v^{DOS} \phi_L^H = -\frac{A_x \phi_0^*}{S_x}\left(\frac{\pi\hbar^2}{m_h^*} + \frac{q^2 \delta_{it}}{\varepsilon_i \varepsilon_0}\right)^{-1}. \tag{33}$$

Here $q^2 m_h^* / \pi\hbar^2$ and $\varepsilon_i \varepsilon_0 / \delta_{it}$ are, respectively, the capacitance per unit area of the density of the valence band near the VBM at the interface and of the interfacial dielectric layer. Hence $(\pi\hbar^2 / q^2 m_h^* + \delta_{it} / \varepsilon_i \varepsilon_0)^{-1}$ denotes the combined capacitance of the two capacitors in series. Besides, $\phi_0^* / S_x = X_m^0 - X_s$ as indicated in Eq. (31). Hence $A_x \phi_0^* / S_x = \phi_0^* / S_\phi$ denotes the energy difference between the metal work function and the diamond VBM $(\phi_m - I_s)$ at the interface in the case where the Fermi level coincides with FL-H ($\approx$FL-H^{free}) as suggested in Fig. 4. This difference corresponds to the bias voltage of the capacitor. From Eq. (33), $qp_{acc} = -(\phi_0^* / qS_\phi)(\pi\hbar^2 / q^2 m_h^* + \delta_{it} / \varepsilon_i \varepsilon_0)^{-1}$ is therefore interpreted as the charge of the capacitor at the diamond side at the bias voltage $-\phi_0^* / qS_\phi$ (note $\phi_0^* < 0$).

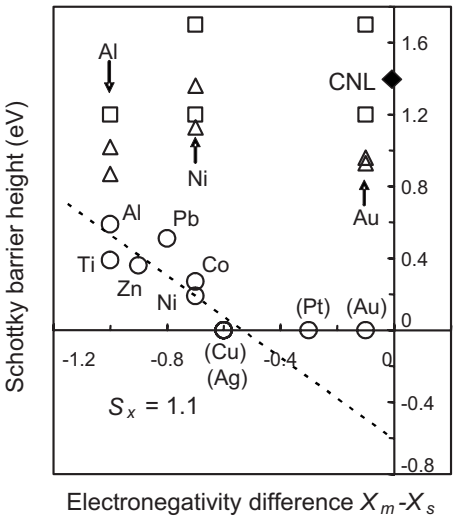

FIG. 5. Schottky barrier heights of metal/diamond contacts plotted vs electronegativity differences between metals (X_m) and diamond (X_s) in Pauling's scale of electronegativities. The open circles (○) denote the data of metal/hydrogen-terminated diamond (001) interfaces measured in this work. The open squares (□) and the open triangles (△) indicate, respectively, the data of metal/oxygen-terminated (001) (Ref. 17) and (111) (Ref. 18) interfaces. A theoretically calculated CNL (1.4 eV from the VBM) (Ref. 48) is also indicated in the figure.

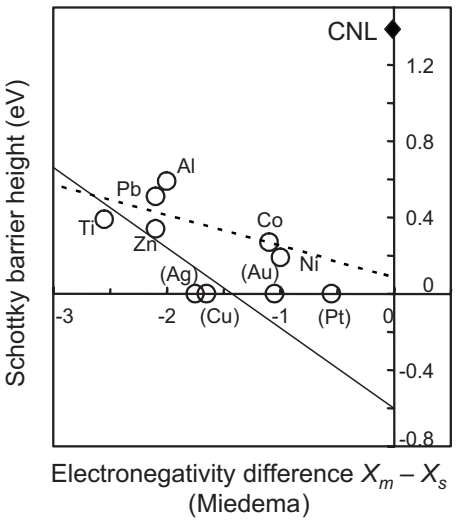

FIG. 6. Experimentally obtained Schottky barrier heights of metal/diamond contacts plotted against electronegativity differences ($X_m - X_s$) in Miedema's electronegativity scale. The dashed line denotes a least-square fit by Schottky contacts (Al, Pb, Zn, Ti, Co, and Ni). The least-square fit by using Pauling's scale Eq. (35), indicated by a dashed line in Fig. 5, corresponds to the solid line in this figure.

When the Fermi level is below the VBM, Q_{ss} and Q_{it} are positive, and from Eq. (6), $Q_{it}=qD_{it}\phi_{\mathrm{CNL}}>Q_{ss}$. Hence the charge-neutrality condition at the free surface Eq. (4) leads to

$$p_{acc} < N_{sa} < p_{acc} + D_{it}\phi_{\mathrm{CNL}}. \tag{34}$$

Since S_x and ϕ_0^* are experimentally obtained, one can estimate the hole sheet density of the surface conductive layer on a hydrogen-terminated diamond surface from Eqs. (33) and (34). Then one can evaluate the electron affinity from the correlation Eq. (24) between N_{sa} and $\Delta\chi_s$.

B. Analysis of experimental results

Figure 5 demonstrates relationship between metal electronegativities and barrier heights of the corresponding metal contacts on the hydrogen-terminated diamond measured in this work. As one can see in the figure, the plotted data displays a linear correlation. In Fig. 5, Pauling's electronegativity scale is used. In dealing with interfaces between solids, generally speaking, Miedema's scale of electronegativities are preferred to Pauling's. This is because Miedema's electronegativities have been derived from properties of solid[49] whereas Pauling's electronegativities are based on chemical-bond energies of small molecules.[50] In this work, however, Miedema's electronegativities give scattered data and poor linearity compared to Pauling's. Figure 6 shows the barrier heights plotted against $X_m - X_s$ in Miedema's scale. In Fig. 6, a linear correlation among the six Schottky contacts can hardly comprise the ohmic contacts (Cu, Ag, Au, and Pt). This situation is in contrast to that in Pauling's scale shown in Fig. 5 as discussed later using the interface model. Pauling's electronegativities are therefore employed hereafter.

Tung[51] has pointed out that the behavior of metal/diamond interfaces, such as S_ϕ in particular, deviates considerably from a trend of other semiconductors using data of the hydrogen-terminated (001) in the literature.[25] He has ascribed the deviation to a higher interface bond density of diamond than other semiconductors since diamond is an elemental semiconductor with a small lattice constant. This may be related to the fact that Pauling's picture works better than Miedema's for the contacts on diamond in this work.

In Fig. 5, a least-squares fit by using the plots of the Schottky contacts of $X_m<1.9$ ($X_m-X_s<-0.6$), i.e., excluding the ohmic contacts, gives the dashed line expressed as

$$\phi_{bp} = -0.6 - 1.1(X_m - X_s)(\mathrm{eV}) \tag{35}$$

with a linear-regression coefficient $r=0.86$. Comparing Eq. (35) with Eq. (15), $S_x=1.1$ and $\phi_0^*=-0.6$ eV are obtained. This value of S_x is slightly larger than those of point contacts (0.7–1.0) in previously reported works.[6,20] Since the S factor is directly related to the density of interface states as suggested in Eq. (13), it is supposed to be sensitive to the preparation of samples. Here the preparation includes the deposition conditions of the diamond homoepitaxial layer, the hydrogen-termination treatment, and the contact (interface) formation. Hence the differences in S factors are considered to be due to the different preparations of the samples and contacts. In addition, the larger S factor here than the previously reported values signifies lower density of interface states of the evaporated contacts in the present work than those of the point contacts in the previous works. Furthermore, an S factor of 1.1 in the present work is much larger than those in other covalent semiconductors, such as Si and Ge ($S_x<0.1$), and comparable to ionic semiconductors ($S_x\approx 1$).[43]

In Miedema's electronegativities, a least-square fit using the six Schottky contacts (Al, Pb, Zn, Ti, Co, and Ni), indicated by the dashed line in Fig. 6, does not work well as aforementioned. In this case, S_x=0.16 and ϕ_0^*=+0.09 with a linear-regression coefficient r=0.66. This MIGS line cannot explain the ohmic contacts (Ag, Cu, Au, and Pt) in Fig. 6, as schematically illustrated in Fig. 4, unlike the MIGS line in Pauling's scale in Fig. 5. Since the parameter A_x is 0.86 for Miedema's scale,[32] S_x of 1.1 in Pauling's scale in Eq. (35) corresponds to 0.42 in Miedema's scale. The MIGS line corresponding to Eq. (35) is drawn by the solid line in Fig. 6. Note that ϕ_0^* is independent of the electronegativity scale. This line can take the ohmic contacts into account though several Schottky contacts, such as Co and Ni, in particular, deviate considerably from it.

The slope parameter, which exhibits controllability of the Fermi level at an interface, is connected to the density of interface states as Eq. (13). Rearranging Eq. (13) gives

$$D_{it} = \frac{(1 - S_\phi)\varepsilon_i \varepsilon_0}{S_\phi \delta_{it} q^2}. \tag{36}$$

The interface layer thickness δ_{it} is expected to have an atomic dimension, i.e., 3 or 5 Å. Assuming δ_{it}=4 Å (Ref. 52) and ε_i=2,[53] and using Eq. (30) with A_x=2.27,[54] the density of the interface states D_{it}, which is equivalent to the density of MIGS for an ideal interface, is estimated at 3.0×10^{13} states/eV cm^2 from Eq. (36). This density is one order of magnitude less than a theoretically calculated value for a jellium/clean diamond (111) interface (2.3×10^{14} states/eV cm^2).[53] In addition, S_x=1.1 is around three times larger than that of a calculated value (0.38) of the jellium/diamond interface. This denotes that the density of the interface states is effectively reduced by hydrogen termination as observed in hydrogen-terminated Si,[55] sulfur-terminated GaAs,[56] or hydrogen-terminated 6H-SiC.[57]

In Fig. 5, barrier heights of Al, Ni, and Au contacts on oxygen-terminated diamond (001) and (111) surfaces are also plotted. The data is taken from the literatures by Takeuchi *et al.*[17] for the (001) and Ri *et al.*[18] for the (111) as examples. As one can see in Fig. 5, the barrier heights of the metal/oxygen-terminated diamond interfaces are independent of the electronegativity of metals, in contrast to the hydrogen-terminated (001). The Fermi levels at the interfaces are strongly pinned at 0.9–1.7 eV from the VBM. As mentioned before, the Fermi level is pinned at or near the CNL of the interface states. The Fermi level of an interface approaches asymptotically its CNL with increasing density of interface states around the CNL without other extrinsic factors such as interface defects, etc. According to the canonical pinning model by Tersoff,[58] the CNL of interface states is identical to the branch point of the complex band structure of a semiconductor, i.e., the position of the CNL in the band gap reflects the bulk band structure of the semiconductor. Hence the energy position of the CNL with respect to the VBM is considered to be independent of the surface termination. Since metal/clean diamond interfaces exhibit an agreement with ϕ_{CNL}=1.4 eV,[25] the CNL of the oxygen-terminated surface may be located at the same position. This roughly agrees with experimental data in Fig. 5 and the literatures.[13–18] For the hydrogen-terminated diamond, ϕ_{CNL}=1.4 eV is therefore assumed in this work.

Substituting the obtained and the assumed numerical data into Eq. (24) gives

$$\Delta\chi_s(\mathrm{eV}) - 1.8\times10^{-14}\times N_{sa}(/\mathrm{cm}^2) = -2.0. \tag{37}$$

Using a density-of-states effective mass of holes $m_h^* \approx 0.8 m_0$ (Ref. 59) for Eq. (33), the inequality Eq. (34) leads to

$$3.2\times10^{13} < N_{sa} < 7.4\times10^{13}(/\mathrm{cm}^2). \tag{38}$$

This result is in good agreements with experimental hole sheet densities by Hall measurements[34,35] ranging from 10^{12} to 10^{14}/cm^2. From Eq. (37), this relation gives

$$-1.4 < \Delta\chi_s < -0.7(\mathrm{eV}). \tag{39}$$

Maier *et al.*[24] have investigated electron affinities χ_s of diamond (001) surfaces by a combination of work function and photoemission experiments. They resulted in χ_s=−1.3 eV for the fully hydrogenated surface and +1.7 eV for the oxidized surface while χ_s=+0.5 eV for the clean surface. Hence the C-H dipole-induced electron affinity lowering $\Delta\chi_s$=−1.8 eV at the minimum. In addition, as-prepared (as hydrogen-plasma treated) specimens exhibited χ_s from −1.0 to −0.6 eV.

Taking an electron affinity of the clean (001) χ_s^{clean} =+0.5 eV, Eq. (39) gives

$$-0.9 < \chi_s^{Hterm} < -0.2(\mathrm{eV}). \tag{40}$$

This roughly agrees with the electron affinities of the as-prepared specimens.

For the clean surface, from Eq. (25), the Fermi-level position with respect to the vacuum level is estimated at $\phi_{sd} = I_s - \phi_{\mathrm{CNL}} = \chi_s^{clean} + E_g - \phi_{\mathrm{CNL}}$=4.6 eV using a band gap E_g =5.5 eV. In addition, substituting the numerical data into Eq. (32) yields ϕ_L^H=−0.1 eV. As pointed out before, assuming that the Fermi-level position of the hydrogen-terminated surface with respect to the vacuum level is identical to ϕ_{sd} of the clean surface, one obtains from Eq. (27)

$$\chi_s^{Hterm} + E_g - \phi_L^H = 4.6(\mathrm{eV}). \tag{41}$$

This results in χ_s^{Hterm}=−0.8 eV. Using this value for Eq. (37), one obtains $N_{sa}=4\times10^{13}$/cm^2. These values reasonably agree with the experimental data, supporting that the assumption on the Fermi-level position. In fact, the MIGS line for the hydrogen-terminated diamond Eq. (23) and the FL-H position Eq. (32) can be mathematically derived from the assumption Eq. (27).

The discussion so far involves the interface between a metal and the hydrogen-terminated diamond (001) surface. However, the interface model built in the present work is not based on the assumption of a specific orientation of diamond. It employs the experimental data obtained on the hydrogen-terminated diamond (001), including the barrier heights, the sheet carrier densities, and the electron-affinity difference $\Delta\chi_s$, for the discussion. The model can therefore be used to analyze an interface on the hydrogen-terminated diamond (111), another typical surface orientation of diamond, by us-

ing data for the (111) surface such as barrier heights of metal contacts,[18] $\Delta\chi_s=1.65$ eV,[23] and so forth. To our knowledge, however, adequate data are not available for analysis of the (111) by using the model at present.

Finally, we would like to consider the hydrogen-terminated free surface illustrated in Fig. 3(a). Supposing the surface negative charge Q_{sa} does not exist on the surface, the surface-charge neutrality Eq. (4) becomes $Q_{ss}+Q_{hole}^{acc}=0$. This condition is satisfied only when $Q_{ss}=Q_{hole}^{acc}=0$. This indicates that the Fermi level coincides with the CNL. Considering the charge of the surface C-H dipole layer Q_{id}, the situation does not change due to the dipole layer is neutral in total. In other words, the net charge on the semiconductor (diamond) side of the dipole layer Q_s is written as

$$Q_s = Q_{ss} + Q_{hole}^{acc} + Q_{id}^{-}, \tag{42}$$

where Q_{id}^{-} denotes the negative contribution of the dipole layer into the diamond surface. On the other hand, the positive contribution of the dipole layer on the other side of the dipole layer Q_{id}^{+} should be in balance with Q_s. Since $Q_{id}^{+}=-Q_{id}^{-}$, $Q_{ss}+Q_{hole}^{acc}=0$ is required.

Once another charge Q_{sa} emerges on the surface, however, the Fermi level moves to satisfy another charge neutrality. If the conservation of ϕ_{sd} is not fortuity, the electron affinity must not change by only the surface dipoles. The existence of negative charge Q_{sa} is required to generate the NEA. However, vice versa, supposing the NEA is only attributed to the surface dipoles, the ϕ_{sd} conservation is brought by Q_{sa}. In whichever case, Q_{sa} is probably determined to maintain the Fermi-level position with respect to the vacuum level.

By annealing the hydrogen-terminated diamond (001) surface in ultrahigh vacuum (UHV) at rising temperatures up to 1050 °C, the electron affinity of the diamond sample reaches +0.5 eV, which is the same value as the clean (001) surface.[24] This fact suggests that $\Delta\chi_s\rightarrow 0$ by the annealing in UHV. During the annealing-process sequence, the surface conduction is expected to vanish.[60] This suggests that $Q_{sa}\rightarrow 0$. Hence the NEA is considered to require Q_{sa} as well as the surface dipoles, i.e., the latter case of the two above.

As expected from Eqs. (23) and (24), a decrease in N_{sa} coinciding with a decrease in $\Delta\chi_s$ gives a barrier-height increase. Annealing in vacuum before measurements possibly causes higher barrier heights than measurements without annealing in some cases. One of the aforementioned reasons for the higher barrier heights in the previous works may be the annealing in vacuum before *I-V* measurements. A recent theoretical study by using the first-principles calculation[61] has revealed that the barrier height of the Al contact on the hydrogen-terminated diamond (001) is 1.1 eV. The model constructed in that work does not include the surface charge Q_{sa}. The resultant barrier height is therefore larger than that in the present work as expected. However tendencies, such as a high S factor ($S_\phi=0.63$) and a low barrier height of the Au contact (0.1 eV), agree with this work.

In the interface of a metal/hydrogen-terminated diamond interface, the conservation is easily realized regardless of Q_{sa} because the presence of the charge on the metal side Q_m with vast density of states around the Fermi level, can compensate the positive contribution of the interface dipole layer Q_{id}^{+}. For other semiconductors, barrier-height variations or CNL deviations may be explained in a similar manner.[45,46,57]

V. SUMMARY

Chemical trends of Schottky barrier heights of ten kinds of metal contacts on hydrogen-terminated (001) surfaces of homoepitaxial CVD diamond were investigated. The barrier heights have been evaluated by temperature dependence of *I-V* characteristics without using contact areas. In addition, the interfaces between metal/hydrogen-terminated diamond contacts are modeled. The correlation among barrier heights, carrier densities, and electron affinities is derived from the model.

The measured barrier heights are lower than those reported previously. However, using the model, estimated carrier densities and electron affinities (NEA) from the experimental barrier heights are coincide well with other experimental data.

ACKNOWLEDGMENTS

This work was supported in part by a Grant-in-Aid for Fundamental Research S (Grant No. 19106006) and by a Grant-in-Aid for Scientific Research S (Grant No. A07102000) from the Ministry of Education, Culture, Sports, Science and Technology (MEXT), Japan.

*k.tsugawa@aist.go.jp

[1] T. Maki, S. Shikama, M. Komori, Y. Sakaguchi, K. Sakuta, and T. Kobayashi, Jpn. J. Appl. Phys., Part 2 **31**, L1446 (1992).
[2] K. Tsugawa, K. Kitatani, H. Noda, A. Hokazono, K. Hirose, M. Tajima, and H. Kawarada, Diamond Relat. Mater. **8**, 927 (1999).
[3] K. Tsugawa, H. Umezawa, and H. Kawarada, Jpn. J. Appl. Phys. **40**, 3101 (2001).
[4] S. A. Grot, G. S. Gildenblat, C. W. Hatfield, C. R. Wronski, A. R. Badzian, T. Badzian, and R. Messier, IEEE Electron Device Lett. **11**, 100 (1990).
[5] M. Tachiki, T. Fukuda, K. Sugata, H. Seo, H. Umezawa, and H. Kawarada, Appl. Surf. Sci. **159-160**, 578 (2000).
[6] H. Kawarada, Surf. Sci. Rep. **26**, 205 (1996).
[7] H. Kawarada, M. Aoki, H. Sasaki, and K. Tsugawa, Diamond Relat. Mater. **3**, 961 (1994).
[8] M. Kasu, Electron. Lett. **41**, 1249 (2005).
[9] H. Taniuchi, H. Umezawa, T. Arima, M. Tachiki, and H. Kawarada, IEEE Electron Device Lett. **22**, 390 (2001).
[10] F. Maier, M. Riedel, B. Mantel, J. Ristein, and L. Ley, Phys. Rev. Lett. **85**, 3472 (2000).
[11] B. Koslowski, S. Strobel, and P. Ziemann, Phys. Rev. Lett. **87**, 209705 (2001).

[12] M. Kasu, K. Ueda, Y. Yamauchi, and T. Makimoto, Appl. Phys. Lett. **90**, 043509 (2007).
[13] G. H. Glover, Solid-State Electron. **16**, 973 (1973).
[14] M. W. Geis, D. D. Rathman, D. J. Ehrlich, R. A. Murphy, and W. Lindley, IEEE Electron Device Lett. **8**, 341 (1987).
[15] H. Shiomi, H. Nakahata, T. Imai, Y. Nishibayashi, and N. Fujimori, Jpn. J. Appl. Phys. **28**, 758 (1989).
[16] K. Hayashi, S. Yamanaka, H. Watanabe, T. Sekiguchi, H. Okushi, and K. Kajimura, J. Appl. Phys. **81**, 744 (1997).
[17] D. Takeuchi, S. Yamanaka, H. Watanabe, and H. Okushi, Phys. Status Solidi A **186**, 269 (2001).
[18] S. G. Ri, D. Takeuchi, N. Tokuda, H. Okushi, and S. Yamasaki, Appl. Phys. Lett. **92**, 112112 (2008).
[19] J. Shirafuji and T. Sugino, Diamond Relat. Mater. **5**, 706 (1996).
[20] M. Aoki and H. Kawarada, Jpn. J. Appl. Phys. **33**, L708 (1994).
[21] F. J. Himpsel, J. A. Knapp, J. A. Van Vechten, and D. E. Eastman, Phys. Rev. B **20**, 624 (1979).
[22] B. B. Pate, Surf. Sci. **165**, 83 (1986).
[23] J. B. Cui, J. Ristein, and L. Ley, Phys. Rev. Lett. **81**, 429 (1998).
[24] F. Maier, J. Ristein, and L. Ley, Phys. Rev. B **64**, 165411 (2001).
[25] W. Mönch, Europhys. Lett. **27**, 479 (1994).
[26] D. Takeuchi, S. Yamanaka, H. Watanabe, H. Okushi, and K. Kajimura, Appl. Surf. Sci. **159-160**, 572 (2000).
[27] S. Yamanaka, H. Watanabe, S. Masai, S. Kawata, K. Hayashi, H. Okushi, and K. Kajimura, J. Appl. Phys. **84**, 6095 (1998).
[28] B. Rezek, C. Sauerer, C. E. Nebel, M. Stutzmann, J. Ristein, L. Ley, E. Snidero, and P. Bergonzo, Appl. Phys. Lett. **82**, 2266 (2003).
[29] C. E. Nebel, B. Rezek, D. Shin, and H. Watanabe, Phys. Status Solidi A **203**, 3273 (2006).
[30] F. A. Padovani and R. Stratton, Solid-State Electron. **9**, 695 (1966).
[31] A. M. Cowley and S. M. Sze, J. Appl. Phys. **36**, 3212 (1965).
[32] W. Mönch, Appl. Surf. Sci. **92**, 367 (1996).
[33] H. Kawarada, H. Sasaki, and A. Sato, Phys. Rev. B **52**, 11351 (1995).
[34] K. Hayashi, H. Yamanaka, S. Okushi, and K. Kajimura, Appl. Phys. Lett. **68**, 376 (1996).
[35] C. E. Nebel, C. Sauerer, F. Ertl, M. Stutzmann, C. F. O. Graeff, P. Bergonzo, O. A. Williams, and R. Jackman, Appl. Phys. Lett. **79**, 4541 (2001).
[36] W. Mönch, Surf. Sci. **299-300**, 928 (1994).
[37] V. Heine, Phys. Rev. **138**, A1689 (1965).
[38] S. G. Louie, J. R. Chelikowsky, and M. L. Cohen, Phys. Rev. B **15**, 2154 (1977).
[39] J. A. Garrido, C. E. Nebel, M. Stutzmann, E. Snidero, and P. Bergonzo, Appl. Phys. Lett. **81**, 637 (2002).
[40] F. Houzé, J. Alvarez, J.-P. Kleider, P. Bergonzo, E. Snidero, and D. Tromson, Diamond Relat. Mater. **15**, 618 (2006).
[41] R. T. Tung, Phys. Rev. B **64**, 205310 (2001).
[42] C. A. Mead, Solid-State Electron. **9**, 1023 (1966).
[43] M. Schlüter, Phys. Rev. B **17**, 5044 (1978).
[44] W. Mönch, Appl. Phys. Lett. **67**, 2209 (1995).
[45] R. F. Schmitsdorf, T. U. Kampen, and W. Mönch, Surf. Sci. **324**, 249 (1995).
[46] T. U. Kampen and W. Mönch, Surf. Sci. **331-333**, 490 (1995).
[47] C. E. Nebel, B. Rezek, and A. Zrenner, Diamond Relat. Mater. **13**, 2031 (2004).
[48] M. Cardona and N. E. Christensen, Phys. Rev. B **35**, 6182 (1987).
[49] A. R. Miedema, P. F. de Châtel, and F. R. de Boer, Physica B (Amsterdam) **100**, 1 (1980).
[50] L. Pauling, J. Am. Chem. Soc. **54**, 3570 (1932).
[51] R. T. Tung, Phys. Rev. Lett. **84**, 6078 (2000).
[52] X. G. Wang and J. R. Smith, Phys. Rev. Lett. **87**, 186103 (2001).
[53] J. Ihm, S. G. Louie, and M. L. Cohen, Phys. Rev. Lett. **40**, 1208 (1978).
[54] W. Gordy and W. J. Thomas, J. Chem. Phys. **24**, 439 (1956).
[55] M. Wittmer and J. L. Freeouf, Phys. Rev. Lett. **69**, 2701 (1992).
[56] J. F. Fan, H. Oigawa, and Y. Nannichi, Jpn. J. Appl. Phys., Part 2 **27**, L2125 (1988).
[57] S. Hara, Surf. Sci. **494**, L805 (2001).
[58] J. Tersoff, Phys. Rev. Lett. **52**, 465 (1984).
[59] A. T. Collins and A. W. S. Wiliams, J. Phys. C **4**, 1789 (1971).
[60] J. Ristein, F. Maier, M. Riedel, J. B. Cui, and L. Ley, Phys. Status Solidi A **181**, 65 (2000).
[61] H. Kageshima and M. Kasu, Jpn. J. Appl. Phys. **48**, 111602 (2009).